

Vulcanian explosion at Soufrière Hills Volcano, Montserrat on March 2004 as revealed by strain data

Linde, Alan T.; Clarke, A. B.; Malin, P.; Shalev, E.; Sparks, S.; Sacks, Selwyn; Hidayat, Dannie;
Voight, Barry; Elsworth, Derek; Mattioli, Glen; Widiwijayanti, Christina

2010

Linde, A. T., Sacks, S., Hidayat, D., Voight, B., Clarke, A. B., Elsworth, D., et al. (2010).
Vulcanian explosion at Soufrière Hills Volcano, Montserrat on March 2004 as revealed by
strain data. *Geophysical research letters*, 37.

<https://hdl.handle.net/10356/95411>

<https://doi.org/10.1029/2009GL041988>

© 2010 American Geophysical Union. This paper was published in *Geophysical Research Letters* and is made available as an electronic reprint (preprint) with permission of American Geophysical Union. The paper can be found at the following official URL: [DOI: <http://dx.doi.org/10.1029/2009GL041988>]. One print or electronic copy may be made for personal use only. Systematic or multiple reproduction, distribution to multiple locations via electronic or other means, duplication of any material in this paper for a fee or for commercial purposes, or modification of the content of the paper is prohibited and is subject to penalties under law.



Vulcanian explosion at Soufrière Hills Volcano, Montserrat on March 2004 as revealed by strain data

Alan T. Linde,¹ Selwyn Sacks,¹ D. Hidayat,² B. Voight,² A. Clarke,³ D. Elsworth,² G. Mattioli,⁴ P. Malin,⁵ E. Shalev,⁵ S. Sparks,⁶ and C. Widiwijayanti²

Received 2 December 2009; revised 22 January 2010; accepted 3 February 2010; published 18 March 2010.

[1] The CALIPSO collaborative volcano monitoring system on the Caribbean island of Montserrat includes observations of strain at depths ~200 m using Sacks-Evertson strainmeters. Strain data for the March 2004 explosion of the Soufrière Hills Volcano are characterized by large, roughly equal but opposite polarity changes at the two near sites and much smaller changes at a more distant site. The strain amplitudes eliminate a spherical pressure (Mogi-type) source as the sole contributor. The initial changes are followed by smaller recoveries, but with differing relative recovery magnitudes. This dissimilarity requires a minimum of two pressure sources, which we model as a deep spherical pressure source and a shallow dike. The spherical source is fixed at the location derived from data for the massive dome collapse in July 2003. We solve for the best fitting dike plus sphere source combination. The dike geometry is consistent with earlier interpretations of dikes based on GPS data and other lines of evidence. **Citation:** Linde, A. T., et al. (2010), Vulcanian explosion at Soufrière Hills Volcano, Montserrat on March 2004 as revealed by strain data, *Geophys. Res. Lett.*, 37, L00E07, doi:10.1029/2009GL041988.

1. Introduction

[2] Strain data were obtained from the Caribbean Andesite Lava Island Precision Seismo-geodetic Observatory, CALIPSO, a volcano monitoring system installed late 2002 and early 2003 for investigations of the dynamics of the Soufrière Hills Volcano (SHV) magmatic activity. The system consists of an integrated array of specialized instruments in four strategically located ~200-m-deep boreholes in concert with several shallower holes and surface sites. CALIPSO was initiated because the volcanic activity was continuing and provided an opportunity to take advantage of the high sensitivity of borehole strain measurements to record data critical for investigating properties of the activity; to the extent that SHV is typical of andesitic dome-building volcanoes, results from this program can be

expected to apply more generally. The borehole sites, at distances of 5.4 to 9.3 km from the crater (Figure 1), include a very broad-band Sacks-Evertson dilatometer, a three-component seismometer, a tiltmeter, and a continuous GPS station at the surface [Mattioli *et al.*, 2004; B. Voight *et al.*, Unique strainmeter observations of Vulcanian explosions, Soufriere Hills Volcano, Montserrat, July 2003, submitted to *Geophysical Research Letters*, 2010, hereinafter referred to as Voight *et al.*, submitted manuscript, 2010]. The dilatometers are high dynamic range deformation detectors capable of recording strain changes as small as 10 picostrain, from 0–20 Hz [Sacks *et al.*, 1971].

2. Background Information About SHV Events

[3] On 12–13 July 2003, after eight years of eruption at SHV, the enormous lava dome (Figure 1) collapsed and generated a series of pyroclastic flows [Herd *et al.*, 2005]. A volume of ~0.2 km³ was involved in the collapse, which lasted several hours. This collapse caused expansion at AIRS & TRNT (strainmeters nearest the vent) and contraction at GERD, consistent with a pressure increase in a moderately deep (~5 km) spherical (Mogi-type) reservoir [Voight *et al.*, 2006].

[4] The collapse triggered several explosions, also recorded by the three operating strainmeters [Mattioli *et al.*, 2004; Linde *et al.*, 2003; Voight *et al.*, submitted manuscript, 2010]. Within a week, a small dome was extruded, 60 m wide and 34 m high (MVO data). For the subsequent 8 months, activity of the volcano was reduced and characterized by only occasional long-period swarms and tremor, spaced weeks to months apart. The explosion of March 3, 2004 followed one of these swarms. The explosion removed the small dome that had grown at the center of the crater after the dome collapse, and produced an ash plume more than 7 km above sea level. A small pyroclastic flow, following the explosion, ran down Tar River valley to the sea. From the plume height, a small erupted volume of about 5.10⁴ m³ DRE can be inferred, although there is large uncertainty in this estimate.

3. Observations of the March 2004 Explosion

[5] The strain data accompanying the explosion (Figure 2) are characterized by a rapid initial phase lasting about 1 minute (Stage 1); during this time the nearest site, AIRS, experiences expansion while the more distant TRNT and GERD undergo contraction. Although the strain data show a very high signal/noise ratio, GPS data shows no corresponding changes above the noise level (this is consistent with our model which produces displacements barely

¹Department of Terrestrial Magnetism, Carnegie Institution of Washington, Washington, D. C., USA.

²College of Earth and Mineral Sciences, Pennsylvania State University, University Park, Pennsylvania, USA.

³Geosciences, Arizona State University, Tempe, Arizona, USA.

⁴Department of Geosciences, University of Arkansas, Fayetteville, Arkansas, USA.

⁵Institute of Earth Science and Engineering, University of Auckland, Auckland, New Zealand.

⁶Department of Earth Sciences, Bristol University, Bristol, UK.

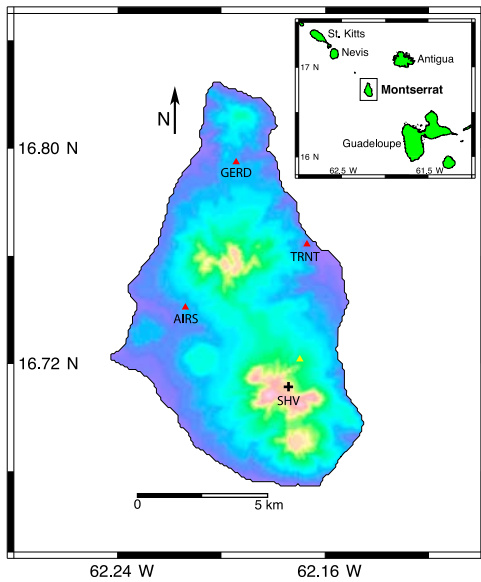


Figure 1. Map of Montserrat showing borehole locations (red triangles) and summit of volcano (SHV, black cross).

above the mm level only in 2 small, un-instrumented, areas). The ~ 30 nanostrain (ns) amplitude at GERD is much smaller than those at AIRS (115 ns) and TRNT (140 ns). During the following ~ 10 minutes (Stage 2) all sites show recovery with AIRS having a much smaller fractional change. Surface manifestations (plume formation) of the event were observed following initiation of Stage 2. Seismic activity begins after observed strain changes, indicating that stresses due to magma movement are responsible for earthquake initiation. Before the rapid initial phase, we do not see any strain changes that can be associated with the explosion.

[6] Stage 1 changes are inconsistent with solely a spherical pressure source [Mogi, 1958] at any depth under the vicinity of the summit: a deep source (>5 km) produces the same sign strain at AIRS and TRNT; a shallower source can cause strain changes of the observed polarity at all sites but cannot produce strain changes at GERD which are much smaller than those at TRNT. Since explosive release of pyroclasts at the surface is observed, there is presumably movement of material (most likely gas because of the short time scales) from a deep reservoir through some conduit towards the surface. The observed strain changes cannot be satisfied by a deep source together with a cylindrical conduit, because they cannot match the polarities observed or the relatively small amplitude noted at GERD. Thus, we look to see if a combination of a spherical reservoir together with a shallow dike can satisfy the data.

4. Analyses: Procedure and Results

[7] Since the event resulted in emission of magmatic material, Stage 1 is presumed to correspond to growth of a dike together with a corresponding loss of pressure in the Mogi reservoir. During Stage 2, which is accompanied by pyroclast ejection and plume formation, the dike partially closes and may be accompanied by some pressure change in the reservoir. Following Voight *et al.* [2006] (see the Introduction), we take the Mogi reservoir to be at 5 km

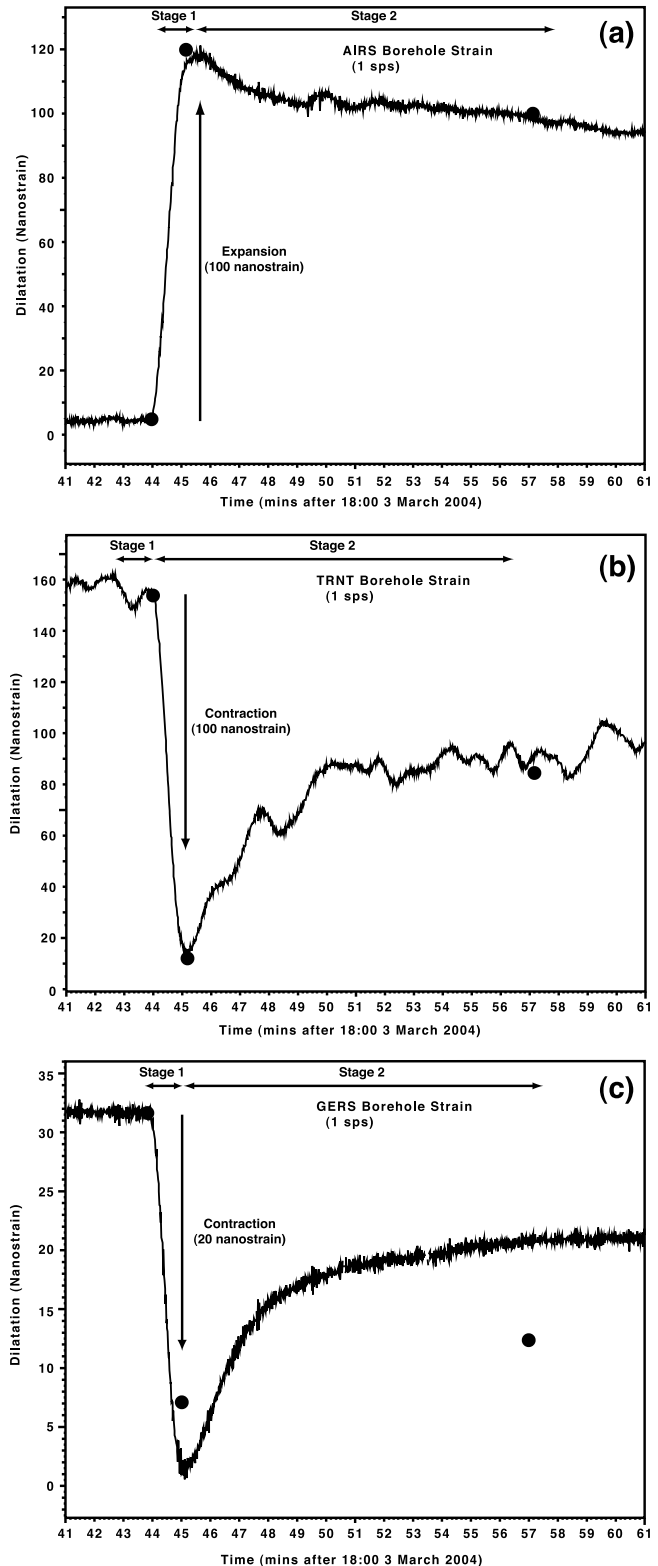


Figure 2. Strain changes generated during the explosion on March 3, 2004 at (a) AIRS, (b) TRNT and (c) GERD. Closed circles show calculated model changes. The model fits the data for AIRS and TRNT extremely well; less so for GERD.

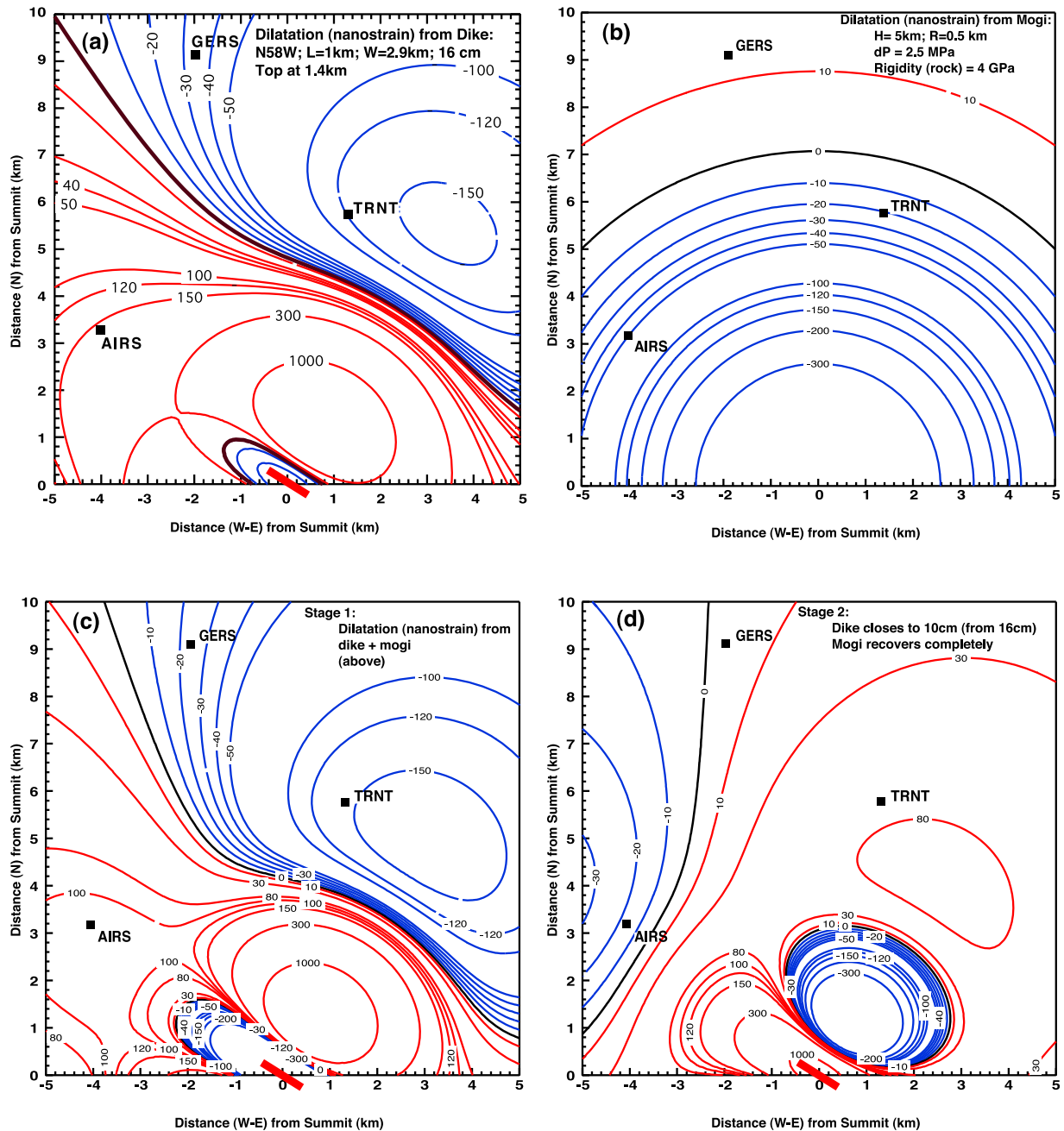


Figure 3. Dilatational strain contours for the preferred model. (a) Strain changes due to dike expansion in Stage 1; (b) Stage 1 Mogi changes; (c) total combined strain changes for Stage 1; (d) combined strain changes for Stage 2. Solid red line at plot origin (volcano summit) indicates model dike. In Figure 3a we see that the 3 sites are located (fortuitously) such that AIRS is most sensitive to the depth to the top of the dike; TRNT amplitude varies strongly with depth to the bottom of the dike and GERS is sensitive to the strike of the dike. Note also that, because of depth dependent nodal lines in the dilatational strain field, a few site measurements of dilatation allow strong control on source parameters.

under the volcano. We can constrain our search for best fitting dike by first looking for numerical solutions to the 2 simple equations for this process:

$$S1(i) = D(i) + M(i)$$

$$S2(i) = F_d * D(i) + F_m * M(i)$$

where $S1(i)$, $S2(i)$ are Stage 1 and 2 strain changes at the i (3) sites; $D(i)$, $M(i)$ are Stage 1 strain changes at the i^{th}

station due to the Mogi source and dike respectively; F_d , F_m are the fractional changes for each source during Stage 2 compared with those for Stage 1.

[8] We carry out a grid point search over the -1 to $+1$ range for both F_d and F_m , solving the two equations for the two unknowns $D(i)$ and $M(i)$ for each station for each grid point; the grid point range thus looks for possible solutions in which either source component can return to its initial state or again have the Stage 1 change. This gives a range of

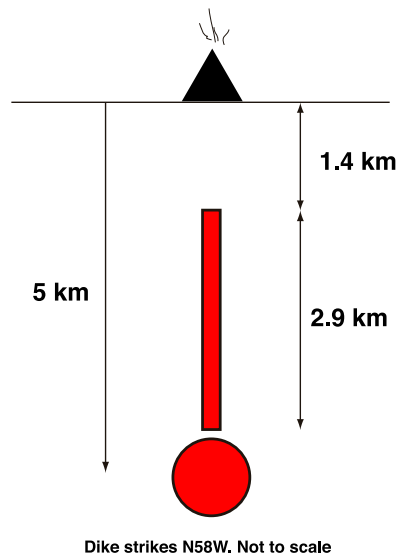


Figure 4. Schematic diagram of model geometry (not to scale). The model comprises a spherical pressure source (Mogi model) with centroid depth 5 km together with a dike that reaches to within 1.4 km of the surface. While some conduit, presumably roughly circular in cross-section, must develop to connect the dike to the surface, model calculations show that the strain changes due to such a shallow source are too small, compared with those due to the dike and Mogi source, to be isolated in our data.

numerical solutions; we accept only those for which the station ratios of the $M(i)$ are in reasonable agreement with a Mogi source at 5 km, as was found for the dome collapse in July 2003, i.e., those are physically acceptable.

[9] This procedure yields a value of -0.4 for F_d and a range for F_m of -0.5 to -1 . Thus, in Stage 2 the dike closes to 0.6 of its Stage 1 opening (Figure 3). The deeper reservoir recovery is constrained to be in the range 0.5 to 1.0. We are able to narrow this range by examining the required dike contributions at the different sites over the range of Mogi recovery. The differing magnitudes contributed by the various recovery possibilities necessarily require different relative, as well as absolute, amplitudes from the dike component. In the context of our modeling, we allow only dikes under the volcano that have a maximum depth not greater than the depth of the reservoir. We find that only recoveries of 0.9 and 1.0 are accompanied by physically realizable dike-produced strain changes. (Our calculations use the formulation developed by Okada [1992].) Over this range there is no significant change in the values of the required strain change due to the dike. For simplicity we take the case of complete Mogi recovery.

[10] We then look for a dike model that produces the strain changes $D(i)$, yielding the results shown in Figures 3 and 4. Our preferred values for the depths to top and bottom of the dike are chosen to be consistent with other information (depth to bottom must be consistent with the location of the reservoir; top depth agrees with estimates of depth extent of the shallow conduit (e.g., Voight et al., submitted manuscript, 2010). Additionally, as can be seen from the contour plots (Figure 3), our strainmeter sites are such that they have different sensitivities to the geometric parameters of the dike. We calculated strain changes due to a variety of models with

varying geometric parameters. From those we see that the ratio of the model dike strain changes at AIRS and TRNT depend on the depths to the top and bottom of the dike; the top of the dike is unlikely to be less than ~ 1 km and cannot be as much as 2 km. GERD model values vary rapidly with strike and require a NW-SE orientation. The model strain values at all sites depend on the product of dike length and opening but these parameters are inseparable; we can vary them over a wide range (e.g., lengths up to several km) without making any obvious changes at our strainmeter sites. Our best fitting model has a vertical dike with orientation about $N60^\circ W$, top at 1.4 km, width (vertical extent) 2.9 km, length along strike 1 km and opening of 16 cm. The length is chosen merely on an intuitive basis as being reasonable but the essence of our conclusions is independent of the precise value. Changes in the length value require changes in the amount of opening (their product must be constant) but has no effect on the depth to top or bottom or on the strike. Note that, in our modeling we do not include any effects due to any conduit connecting the sub-surface dike to the surface. Test calculations for a vertical prolate (cigar-shaped) spheroid [Davis, 1986; Yang et al., 1988] show that strain changes at our sites due to such a very shallow site are very small compared with the observations. Perhaps inclusion of such a source might allow some improvement in the goodness of the fit of the model to the data but at the expense of introducing a number of unconstrained parameters; the basic framework of our model would be unchanged.

5. Discussion

[11] The northwest-southeast orientation and location of the dike in our best-fit model is generally consistent with local geological structures [Harford et al., 2002; C. L. Kenedi et al., Active faulting and oblique extension influence volcanism on Montserrat (West Indies): Evidence from offshore seismic reflection profiles, submitted to *Geophysical Research Letters*, 2010] with seismicity [Miller et al., 2006], and with previous models published by Mattioli et al. [1998] and Hautmann et al. [2009] based on early GPS and tilt data respectively. Note that we do not propose that the dike formed during the 1 minute of Stage 1. It is likely that the dike preexisted (having formed over a much longer interval) and that the dike opening increased rather rapidly just before the explosion.

[12] Green and Neuberg [2005] used broadband seismic data to study the March 2004 explosion and, based on a 120 s dominant period in the seismic data, concluded that the source was a collapse in the shallow part of a conduit, about 300 m below the surface (~ 350 m above sea level). Their two sites were much closer to the volcano (closest 1.6 km) and respond more strongly to changes in the conduit; additionally the initiation of the seismic signal is delayed by ~ 30 seconds compared with the strain signal. Our sites, at much greater distances, are not very sensitive to very shallow sources. Thus analysis of the seismic data provides information complementary to that from the strain data. Strainmeter data encompass a much broader frequency band and clearly show much longer period changes, including a strain offset at all sites, i.e., a large zero frequency component. Importantly, it is impossible to satisfy the strain data with only such a shallow source. GPS

instrumentation does not have sufficient sensitivity to record event-produced displacements above the noise level.

[13] This explosion in March of 2004 differs significantly from those in July of 2003 following the massive dome collapse. For those earlier events, all strain sites experienced contraction (negative strain) (Voight et al., submitted manuscript, 2010), whereas in March of 2004 AIRS (the nearest site) showed expansion. The events in July 2003 produced much smaller strain changes at all sites and can be satisfied by a relatively shallow (cylindrical) conduit source. The March 2004 data are not satisfied by a very shallow source (and indeed shallow strain sources are ignored here because any associated strains are small compared with those actually observed). There must of course be a path to the surface in order for material to escape to form the observed plume; strain changes due to such a shallow source are much smaller than those observed and are not isolated in our modeling. Because of the short time scales for the event, we infer that gas must play a major role although we have no data that bears directly on that aspect.

[14] **Acknowledgments.** This research was supported by National Science Foundation, Continental Dynamics, and Instrumentation and Facilities Programs. Additional support was provided by host institutions of the CALIPSO Consortium, and the Montserrat Volcano Observatory. Helpful comments from two anonymous reviewers led to improvements in the manuscript.

References

- Davis, P. M. (1986), Surface deformation due to inflation of an arbitrarily oriented triaxial ellipsoidal cavity in an elastic half-space, with reference to Kilauea Volcano, Hawaii, *J. Geophys. Res.*, *91*(B7), 7429–7438, doi:10.1029/JB091iB07p07429.
- Green, D. N., and J. Neuberg (2005), Seismic and infrasonic signals associated with an unusual collapse event at the Soufrière Hills volcano, Montserrat, *Geophys. Res. Lett.*, *32*, L07308, doi:10.1029/2004GL022265.
- Harford, C. L., M. S. Pringle, R. S. J. Sparks, and S. R. Young (2002), The volcanic evolution of Montserrat using $^{40}\text{Ar}/^{39}\text{Ar}$ geochronology, in *The Eruption of Soufrière Hills Volcano, Montserrat, From 1995 to 1999*, edited by T. H. Druitt and B. P. Kokelaar, *Geol. Soc. London Mem.*, *21*, 93–114.
- Hautmann, S., J. Gottsmann, R. S. J. Sparks, A. Costa, O. Melnik, and B. Voight (2009), Modelling ground deformation caused by oscillating overpressure in a dyke conduit at Soufrière Hills Volcano, Montserrat, *Tectonophysics*, *471*, 87–95, doi:10.1016/j.tecto.2008.10.021.
- Herd, R., M. Edmonds, and V. A. Bass (2005), Catastrophic lava dome failure at Soufrière Hills Volcano, Montserrat, 12–13 July 2003, *J. Volcanol. Geotherm. Res.*, *148*(3–4), 234–252, doi:10.1016/j.jvolgeores.2005.05.003.
- Linde, A., et al. (2003), Borehole strainmeters on Montserrat: The CALIPSO project and the July 2003 eruption, *Eos Trans. AGU*, *84*(46), Fall Meet. Suppl., Abstract V51J-0407.
- Mattioli, G., T. H. Dixon, F. F. Farina, E. S. Howell, P. E. Jansma, and A. L. Smith (1998), GPS measurement of surface deformation around Soufrière Hills Volcano, Montserrat, from October 1995 to July 1996, *Geophys. Res. Lett.*, *25*(18), 3417–3420, doi:10.1029/98GL00931.
- Mattioli, G. S., et al. (2004), Prototype PBO instrumentation of CALIPSO project captures world-record lava dome collapse on Montserrat Volcano, *Eos Trans. AGU*, *85*(34), doi:10.1029/2004EO340001.
- Miller, V. L., C. Ammon, B. Voight, and G. Thompson (2006), Precise hypocenter location of high-frequency-onset earthquakes during the initial stages of activity at Soufrière Hills Volcano, Montserrat, *Eos Trans. AGU*, *87*(52), Fall Meeting Suppl., Abstract V11B-0586.
- Mogi, K. (1958), Relations between the eruptions of various volcanoes and the deformations of the ground surfaces around them, *Bull. Earthquake Res. Inst. Univ. Tokyo*, *36*, 99–134.
- Okada, Y. (1992), Internal deformation due to shear and tensile faults in a half-space, *Bull. Seismol. Soc. Am.*, *82*, 1018–1040.
- Sacks, I. S., S. Suyehiro, D. W. Everton, and Y. Yamagishi (1971), Sacks-Everton strainmeter: Its installation in Japan and some preliminary results concerning strain steps, *Pap. Meteorol. Geophys.*, *22*, 195–208.
- Voight, B., et al. (2006), Unprecedented pressure increase in deep magma reservoir triggered by lava-dome collapse, *Geophys. Res. Lett.*, *33*, L03312, doi:10.1029/2005GL024870.
- Yang, X.-M., P. M. Davis, and J. H. Dieterich (1988), Deformation from inflation of a dipping finite prolate spheroid in an elastic half-space as a model for volcanic stressing, *J. Geophys. Res.*, *93*(B5), 4249–4257, doi:10.1029/JB093iB05p04249.
- A. Clarke, Geosciences, Arizona State University, Box 871404, Tempe, AZ 85287, USA.
- D. Elsworth, D. Hidayat, B. Voight, and C. Widijayanti, College of Earth and Mineral Sciences, Pennsylvania State University, University Park, PA 16802, USA.
- A. T. Linde and S. Sacks, Department of Terrestrial Magnetism, Carnegie Institution of Washington, 5241 Broad Branch Rd. NW, Washington, DC 20015, USA. (alinde@dtm.ciw.edu)
- P. Malin and E. Shalev, Institute of Earth Science and Engineering, University of Auckland, Private Bag 92019, Auckland 1142, New Zealand.
- G. Mattioli, Department of Geosciences, University of Arkansas, 113 Ozark Hall, Fayetteville, AR 72701, USA.
- S. Sparks, Department of Earth Sciences, Bristol University, Wills Memorial Building, Queen's Road, Bristol BS8 1RJ, UK.